Modeling the concentration dependence of diffusion in zeolites. III. Testing mean field theory for benzene in Na–Y with simulation

Chandra Saravanan and Fabien Jousse
Department of Chemistry, University of Massachusetts, Amherst, Massachusetts 01003

Scott M. Auerbach[a)]
Department of Chemistry and Department of Chemical Engineering, University of Massachusetts, Amherst, Massachusetts 01003

(Received 25 August 1997; accepted 20 October 1997)

We have performed kinetic Monte Carlo (KMC) simulations of benzene tracer diffusion in Na–Y for various loadings and temperatures to test the analytical diffusion theory presented in Paper I of this series. Our theory and simulations assume that benzene molecules jump among S_{II} and W sites, located near Na^+ ions in 6-rings and in 12-ring windows, respectively. Our diffusion theory is based on a mean field approximation (MFA) which yields $D_\theta = \frac{1}{6}k_\theta a_\theta^2$, where $a_\theta \cong 11$ Å is the mean intercage jump length and $1/k_\theta$ is the mean supercage residence time. KMC simulations of $D(\theta)$, k_θ, and a_θ at 300 and 400 K show that our MFA is essentially exact for loadings that allow S_{II} site vacancies, and that the concentration dependence is controlled by k_θ. For higher loadings, the MFA error is independent of temperature, and increases roughly linearly with loading to a maximum value of ca. 25%, resulting from correlated motion. We present an analytical theory for such correlated motion at infinite vacancy dilution, which predicts the corresponding KMC simulated diffusivities to within statistical Monte Carlo error. © *1998 American Institute of Physics.* [S0021-9606(98)50205-X]

I. INTRODUCTION

Significant effort has been devoted to understanding diffusion in zeolites,[1,2] since transport properties play a central role in catalytic and separation processes[3] using zeolites.[4] Understanding the diffusion of aromatics in faujasite type zeolites[5–13] is particularly important because of persistent discrepancies among different experimental probes of mobility.[1,13] We have recently reported the results of analysis and simulation that greatly simplify our picture of benzene tracer diffusion in Na–Y, by focusing on the dynamics of cage-to-cage motion.[12,14–20] Cage-to-cage migration is illustrated in Fig. 1, which shows the tetrahedral connectivity of supercages in Na–Y. In Paper I of this series,[18] we derive simple analytical expressions for the temperature and loading dependence of benzene diffusion in Na–Y. In the present article we report the results of kinetic Monte Carlo (KMC) simulations[12,21,22] of benzene diffusion in Na–Y at finite loadings to test theoretical assumptions made in Paper I.

Our tracer diffusion theory is based on a mean field approximation (MFA) which assumes that instantaneous benzene occupancies in different Na–Y supercages are identical. This yields $D_\theta = \frac{1}{6}k_\theta a_\theta^2$, where $a_\theta \cong 11$ Å is the mean intercage jump length and $1/k_\theta$ is the mean supercage residence time. We note that the expression $D_\theta = \frac{1}{6}k_\theta a^2$ is sometimes assumed[1] to be exact for jump diffusion in cage-type zeolites. Below we will show that our MFA gives quantitative agreement with simulation for low to moderate loadings, and deviates from simulation at high loadings by no more than 25%. As such, these KMC simulations will demonstrate that, while $D_\theta = \frac{1}{6}k_\theta a^2$ can be a very useful formula, it is indeed only an approximate one.

Pulsed field gradient (PFG) NMR diffusivities for aromatics at high loadings in Na–X decrease rapidly with concentration.[23] This effect has been attributed to the diminution of molecular free volume in Na–X leading to reduced mean jump lengths and hence to smaller diffusion coefficients.[23] Our simulation results will suggest that this interpretation may need to be reconsidered. Indeed, our results will show that the mean intercage jump length *increases* with loading. This finding implies that the loading dependence of PFG NMR diffusivities is controlled instead by the cage-to-cage rate coefficient.

Our MFA neglects statistical correlation between jumps when, e.g., a random walker jumps into a W site separating nearly empty and full cages. The next jump for that random walker, although uncorrelated from the last jump in the sense of Poisson statistics, is more likely to end up in the nearly empty cage. In the absence of percolation[24] these correlation effects can be relatively minor; they are nonetheless interesting from a theoretical viewpoint. Below we present an analytical theory for such correlated motion at infinite vacancy dilution, which predicts the corresponding KMC simulated diffusivities to within statistical Monte Carlo error.

The remainder of this paper is organized as follows: In Sec. II we review our analytical diffusion theory, in Sec. III we discuss the simulation methodology and convergence properties, and in Sec. IV we discuss the resulting concentration and temperature dependence of $D(\theta)$, k_θ, and a_θ. In Sec. V we present our theory of correlated motion, and in Sec. VI we conclude by speculating on the applicability of

a)Author to whom correspondence should be addressed.

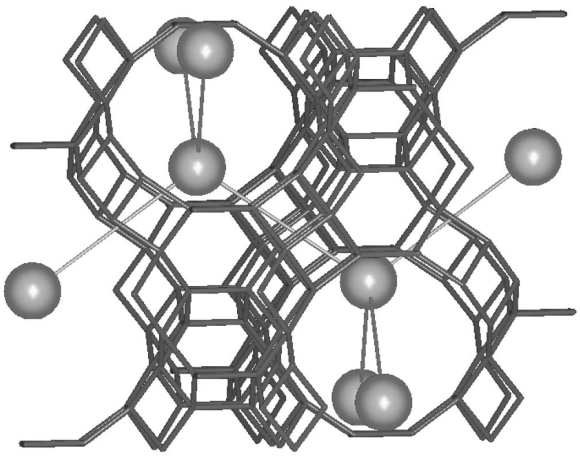

FIG. 1. Tetrahedral connectivity of supercages in the Na–Y unit cell. Balls represent supercage ''sites'' and sticks represent cage-to-cage jumps.

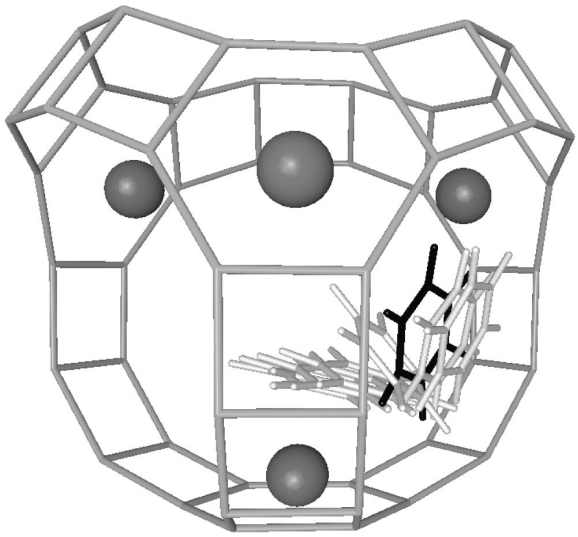

FIG. 2. $S_{II} \leftrightarrow W$ minimum energy path with transition state indicated in bold.

his approach for modeling other host–guest diffusion systems.

II. REVIEW OF ANALYTICAL DIFFUSION THEORY

A. Mean field lattice model

We model benzene tracer diffusion in Na–Y by replacing the zeolite framework with a three-dimensional lattice of binding sites. In this system benzene has two predominant binding sites.[8,12,15] In the primary site, denoted as S_{II}, benzene is facially coordinated to a supercage 6-ring, 2.70 Å above Na(II). In the secondary site, denoted as W, benzene is centered in the 12-ring window separating adjacent supercages, ca. 5.3 Å from the S_{II} site. Figure 2 shows a minimum energy hopping path connecting the S_{II} and W sites.[12] Binding sites at Na(I), Na(I′), and Na(III) are not included in our model because Na(III) is negligibly occupied in Na–Y (Si:Al $=2.0$), and because benzene cannot enter the smaller sodalite cages or hexagonal prisms containing Na(I′) and Na(I) cations, respectively.

The lattice of benzene binding sites in Na–Y is depicted schematically in Fig. 3, with cubes representing supercages and cube vertices representing binding sites. Figure 3 shows that each Na–Y supercage contains four tetrahedrally arranged S_{II} sites and four tetrahedrally arranged, doubly shared W sites. The jump connectivity among sites in our model can be understood from Fig. 3 by allowing jumps along cube edges ($S_{II} \leftrightarrow W$) and along cube face-diagonals ($S_{II} \leftrightarrow S_{II}$ and $W \leftrightarrow W$). Jumps along cube diagonals are not included because the supercage center presents a rather high-energy configuration.

Our tracer diffusion theory[18] is based on a mean field approximation (MFA) which assumes that instantaneous benzene occupancies in different Na–Y supercages are identical. This idea is schematically illustrated in Fig. 4, showing in (a) an instantaneous configuration of benzenes at a certain loading with either completely filled or empty sites. Figure 4(b) illustrates mean field theory at the same loading as (a), with all sites equivalent and partially blocked. When applied to calculating the diffusion coefficient,[18] this MFA yields $D(\theta) = \frac{1}{6} k_\theta a_\theta^2$, where a_θ is the mean intercage jump length and $1/k_\theta$ is the mean supercage residence time. In this section we review our analytical theory for k_θ,[18] and discuss its agreement with previous kinetic Monte Carlo (KMC) simulations.[19]

B. Supercage residence times

In Paper I we showed that $k_\theta = \kappa \cdot k_1 \cdot P_1$, where $P_1 = [1 + K_{eq}(1 \rightarrow 2)]^{-1}$ is the probability of occupying a W site, $\langle \tau_1 \rangle = 1/k_1$ is the mean W site residence time, and κ is the transmission coefficient for cage-to-cage motion.[18] Our theory thus provides a picture of cage-to-cage motion involving transition state theory ($k_1 \cdot P_1$) with dynamical corrections (κ). For consistency with our earlier MFA, we assumed that $\kappa = \frac{1}{2}$ for all loadings. We further assumed that occupancies at S_{II} and W sites are either 0 or 1, and that benzenes do not otherwise interact. We call this assumption the site blocking model. Finally, we allowed at most one W site occupant when some S_{II} sites are vacant, motivated by

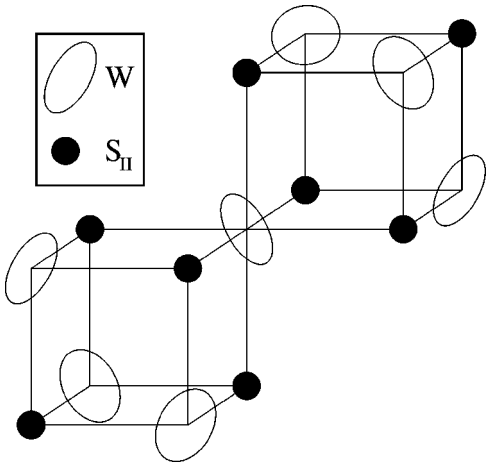

FIG. 3. Schematic of benzene site lattice in Na–Y: cubes represent supercages and cube vertices represent binding sites.

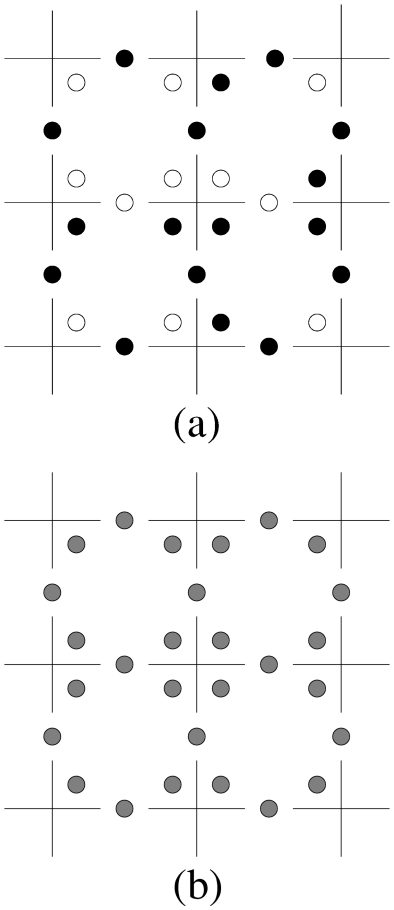

FIG. 4. Two-dimensional schematic of Na–Y: (a) Shows an instantaneous configuration of benzenes at a certain loading. Black circles indicate blocked sites while empty circles show unoccupied sites. (b) Illustrates mean field theory at the same loading as (a), by showing partially blocked sites with gray circles.

the greater stability of S_{II} sites. We call this last assumption the leading order approximation. With these assumptions, we derived the temperature and loading dependence of k_1 and P_1,[18] giving the following formulas for k_θ:

$$k_\theta \cong \frac{3}{2}\left(\frac{N_2}{N_2-N+1}\cdot\frac{k_{1\to1}}{k_{1\to2}}+1\right)k_{2\to1}, \quad \text{for } N\leqslant N_2 \tag{2.1}$$

$$\overset{V\to\infty}{\to} \frac{3}{2}\left(\frac{2}{2-3\theta}\cdot\frac{k_{1\to1}}{k_{1\to2}}+1\right)k_{2\to1}, \quad \text{for } \theta<\frac{2}{3} \tag{2.2}$$

$$\cong 3\left(\frac{N_1+N_2-N}{N_1-1}\right)\left(\frac{N-N_2}{N}\right)k_{1\to1}, \quad \text{for } N>N_2 \tag{2.3}$$

$$\overset{V\to\infty}{\to} 3\,(1-\theta)\left(\frac{3\theta-2}{\theta}\right)k_{1\to1}, \quad \text{for } \theta>\frac{2}{3}. \tag{2.4}$$

In Eqs. (2.1)–(2.4), $\{k_{i\to j}\}$ are site-to-site hopping rate coefficients where the W and S_{II} sites are denoted sites 1 and 2, respectively. The fractional loading is $\theta = 2N/3N_2$ where N is the number of benzene molecules, and $N_2 = 2N_1$ is the total number of Na(II) cations in the model zeolite.

In Paper II we reported KMC simulations of benzene diffusion in Na–Y for comparison with Eqs. (2.1) and (2.3). Since these formulas follow from assuming that benzenes block sites but do not otherwise interact, the KMC simulations used fundamental hopping rate coefficients calculated at infinite dilution to determine jump times and probabilities.[19] We found that Eqs. (2.1) and (2.3) give excellent agreement with KMC simulations of k_θ for all temperatures and loadings studied.[19] As discussed in Paper I, these formulas are accurate up to $T \lesssim 600$ K and $V \lesssim 100$ Na–Y unit cells, using the rate parameters in Paper I. The formulas become slightly less accurate for higher T and V as the leading order approximation begins to break down. Having established the accuracy of our analytical formulas for k_θ, we investigate in the following sections the accuracy of our overall MFA, i.e., $D(\theta) \cong \frac{1}{6}k_\theta a_\theta^2$.

III. SIMULATION METHODOLOGY AND CONVERGENCE

In this article we perform kinetic Monte Carlo (KMC) simulations of benzene tracer diffusion in Na–Y to test the mean field approximation (MFA) yielding $D(\theta) \cong \frac{1}{6}k_\theta a_\theta^2$, by simulating $D(\theta)$, k_θ, and a_θ. The KMC simulations of k_θ presented below are performed exactly as described in Paper II.[19] Please see Ref. 19 for all computational details, including the fundamental rate parameters used below. For completeness, we briefly review the KMC calculation of k_θ and a_θ.

In Paper I we obtain an analytical expression for k_θ by assuming that S_{II} and W site occupancies are either 0 or 1 and that benzenes do not otherwise interact.[18] For consistency, the KMC simulations presented below use fundamental hopping rate coefficients calculated at infinite dilution.[12] The simulation cell is one Na–Y unit cell with periodic boundary conditions, containing 32 S_{II} sites and 16 W sites. For each molecule in the many benzene KMC simulation, we define cage-to-cage jumps, each with a particular hopping length λ and cage residence time τ. Intercage jumps are defined as follows: if the nth KMC step of the ith molecule is a W site, we calculate the distance between benzene center of mass positions for KMC steps $n-1$ and $n+1$. If this distance is nonzero and different from characteristic intracage distances[8] [$d(S_{II},S_{II})=5.48$ Å, $d(S_{II},W)=5.31$ Å, $d(S_{II},W')=8.74$ Å, and $d(W,W)=8.79$ Å], a cage-to-cage jump is registered with t_{n+1} and $\vec{r}_i(n+1)$ stored as the arrival time and position in the new cage, respectively. The residence time τ is the difference between t_{n+1} and the previously stored arrival time, while the intercage jump length λ is the three-dimensional norm of $\vec{r}_i(n+1)$ minus the previously stored arrival position. These quantities are averaged for each molecule over all time steps in a KMC run to yield $k_\theta = 1/\langle\tau\rangle$ and $a_\theta^2 = \langle\lambda^2\rangle$. A convergence criterion is that all molecules have essentially identical values of k_θ and a_θ.

Given a set of fundamental hopping processes and rates, ''exact'' diffusion coefficients can be obtained from a KMC calculation of the mean square displacement (MSD). For the ith molecule, we obtain the diffusion coefficient according to $D_i(\theta) = \lim_{t\to\infty}\langle|\vec{r}_i(t)-\vec{r}_i(0)|^2\rangle/6t$, where $\vec{r}_i(t)$ is the center of mass position of the ith molecule at time t. The ensemble

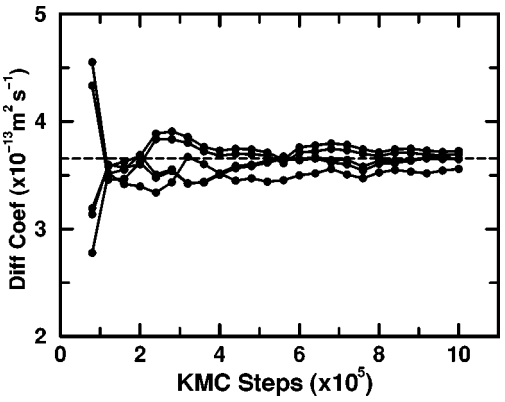

FIG. 5. Convergence of diffusion coefficients with number of KMC steps at 300 K for five molecules per unit cell. Diffusion coefficients are calculated from mean square displacements, and vary by less than 2% after 10^6 KMC steps.

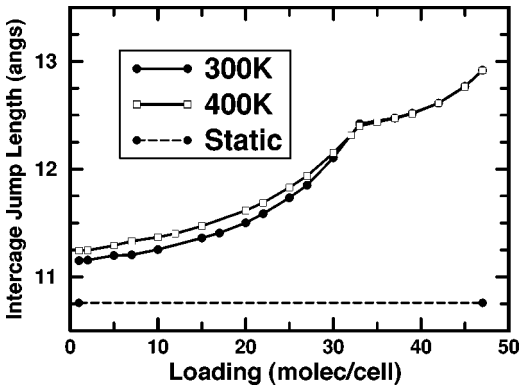

FIG. 6. Intercage jump length versus loading, calculated from KMC for 300 and 400 K, compared to the static intercage distance.

average $\langle \cdots \rangle$ is calculated by multiple-time-step, multiple-time-origin analysis of a single random walk.[12] In this approach, we first choose a time bin width, Δt_{bin}, usually a fraction of the estimated mean supercage residence time. For the time $t=n\Delta t_{bin}$, the mean square displacement of the ith molecule is given by

$$\langle \mathscr{R}_i^2(n\Delta t_{bin})\rangle = \frac{1}{Q_i(n)}\sum_{lm}{}' \, |\vec{r}_i(l)-\vec{r}_i(m)|^2, \tag{3.1}$$

where $\vec{r}_i(l)$ is the center of mass benzene position of molecule i at the KMC time t_l. The sum is restricted to those pairs (l,m) for which t_l-t_m falls into the nth time bin, characterized by $n=\mathrm{int}[(t_l-t_m)/\Delta t_{bin}]$, and $Q_i(n)$ is the number of such pairs. The diffusion coefficient for a particular loading is then obtained by averaging the individual molecular diffusivities once these have reached satisfactory convergence.

Figure 5 shows the convergence of diffusion coefficients with the number of KMC steps at 300 K for 5 molecules per unit cell. These diffusion coefficients are calculated from mean square displacements, and vary by less than 2% after 10^6 KMC steps. At this loading, we can accurately average the MSD up to 3000 Å^2 with 10^6 KMC steps, requiring less than 14 CPU minutes per loading on an IBM RS/6000 PowerPC 604e 200 MHz processor. Longer KMC runs were required for loadings above $N=32$, in order to ensure that sufficient exchange between S_{II} benzenes and W benzenes is obtained. At these higher loadings, 10^8 KMC steps were required for convergence, requiring 8 CPU hours on an IBM RS/6000 PowerPC.

IV. RESULTS AND DISCUSSION

In this section we discuss KMC calculations of $D(\theta)$, k_θ, and a_θ, to test the MFA yielding $D(\theta) \cong \frac{1}{6}k_\theta a_\theta^2$. Before comparing diffusion coefficients, we show in Fig. 6 the simulated concentration and temperature dependence of the intercage jump length, a_θ. Several remarks can be made about Fig. 6. First, a_θ is greater than the static intercage distance 10.76 Å,[8] between adjacent supercage centers, for all loadings and temperatures studied. This reflects the fact that, on average, molecules enter and exit cages through different W sites. Second, a_θ increases monotonically with loading, with an apparent cusp at 33 molecules per unit cell, due to the finite simulation size. Increasing loading populates W sites, from which the longer $(\mathrm{W})_{cage\,1}\rightarrow(\mathrm{S_{II}}$ or $\mathrm{W})_{cage\,2}$ intercage jumps can occur. Third, a_θ increases weakly with temperature for loadings less than 32 molecules per unit cell, also because of enhanced W site population. The temperature dependence of a_θ above 32 molecules per unit cell is negligible since filling S_{II} sites makes the population of W sites nearly temperature independent.[18]

Pulsed field gradient (PFG) NMR diffusivities for aromatics at high loadings in Na–X decrease exponentially with concentration.[23] This effect has been attributed to the diminution of molecular free volume in Na–X leading to reduced mean jump lengths and hence to smaller diffusion coefficients.[23] Our simulation results suggest that this interpretation may need to be reconsidered. Indeed, our present results show that the mean intercage jump length *increases* with loading for the reasons indicated above. This finding implies that the loading dependence of PFG NMR diffusivities is controlled instead by the cage-to-cage rate coefficient. In a forthcoming publication we will explore how the loading dependence of a_θ is modified by including the full effect of guest–guest interactions.[25]

Figure 7 shows a comparison of tracer diffusion coefficients from (i) our analytical expression for k_θ and $a_\theta = 11$ Å (MFA1), (ii) simulated values for k_θ and a_θ (MFA2), and (iii) MSD calculations. Figure 7 demonstrates excellent quantitative agreement among all three levels of theory for benzene diffusion in Na–Y. Since MFA1 assumes a constant intercage jump length, Fig. 7 shows that the concentration dependence of benzene diffusion in Na–Y is controlled almost exclusively by the cage-to-cage rate coefficient, k_θ. A detailed discussion of the loading dependence of k_θ has been given in Papers I and II in the context of our present site blocking model.[18,19] For completeness, the loading dependence of k_θ is briefly discussed below.

According to our site blocking model, i.e., Eqs. (2.1)–(2.4), k_θ increases at low loadings because of an entropic preference for occupying W sites as S_{II} sites become

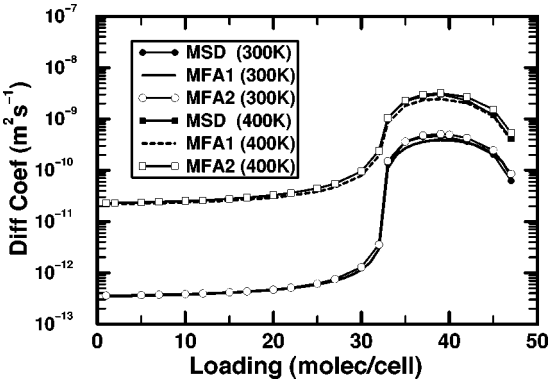

FIG. 7. Diffusion coefficients versus loading for 300 and 400 K, calculated by three methods listed in Table I.

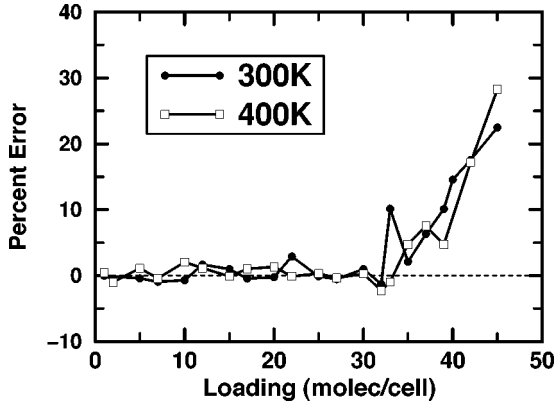

FIG. 8. Percent error between MFA and MSD diffusion coefficients, evaluated as $(D_{\mathrm{MFA2}}-D_{\mathrm{MSD}})/D_{\mathrm{MSD}}\times 100\%$.

blocked. Diffusion within the site blocking model becomes precipitously faster above $\theta=\frac{2}{3}$ as molecules are forced to occupy W sites, i.e., the operative temperature dependence changes from $k_{2\rightarrow 1}$ to $k_{1\rightarrow 1}$. At the highest loadings, as almost all W sites become occupied, the W site residence time increases and slows diffusion. Comparison between site blocking theory and tracer zero-length column data[26] shows excellent qualitative agreement, with $\log D_\theta \propto \theta$ for low to moderate loadings. Comparing our theoretical results with PFG NMR[23] and with frequency response data[27] yields qualitative disagreement in the loading dependence. Kärger and Ruthven have recently reviewed this discrepancy in Ref. 13. In a forthcoming publication we will explore how the loading dependence of our predicted k_θ is modified by including the full effect of guest–guest interactions.[25]

Assuming normal diffusion holds, a rigorous measure of the error associated with our MFA is obtained by comparing MFA2 and MSD diffusivities. Figure 8 shows the loading and temperature dependence of $\mathscr{E}_{\mathrm{MFA}}\equiv(D_{\mathrm{MFA2}}-D_{\mathrm{MSD}})/D_{\mathrm{MSD}}\times 100\%$ for data in Fig. 7. Figure 8 suggests that the magnitude and concentration dependence of $\mathscr{E}_{\mathrm{MFA}}$ is independent of temperature. We return to this issue below. For loadings less than 33 molecules per unit cell, $\mathscr{E}_{\mathrm{MFA}}$ is comparable to the statistical Monte Carlo error in simulated quantities. This suggests that our MFA is essentially *exact* when some S_{II} sites are vacant. For loadings greater than 32 molecules per unit cell, $\mathscr{E}_{\mathrm{MFA}}$ increases roughly linearly with loading to a maximum value of ca. 25%. This error arises because the MFA neglects correlated motion, which becomes important at higher loadings. In the next section we explore methods for treating correlated motion in the limit of infinite vacancy dilution.

We note that the expression $D_\theta=\frac{1}{6}k_\theta a^2$ is sometimes assumed[1] to be exact for jump diffusion in cage-type zeolites. While our present results suggest that this can be a very useful formula, it is indeed only an approximate one.

V. THEORY OF CORRELATED MOTION

Correlation effects have been recognized as playing an important role in the diffusion of vacancies in solids,[28] and quite an extensive body of work has been aimed at defining and calculating exactly these effects.[29,30] Although a number of procedures exist for treating correlated motion at infinite vacancy dilution,[29,31–33] its dependence with vacancy concentration is more difficult to obtain.[30,32,34,35] Therefore we will limit ourselves to the treatment of correlated motion in the limit of infinite vacancy dilution.

The mean square displacement (MSD) of a molecule after N jumps is given by[29]

$$\langle \mathscr{R}^2(N)\rangle=\left\langle \left|\sum_{n=1}^{N}\vec{\boldsymbol{r}}(n)\right|^2\right\rangle=\sum_{n=1}^{N}\langle|\vec{\boldsymbol{r}}(n)|^2\rangle + 2\sum_{n=1}^{N-1}\sum_{n'=1}^{N-n}\langle \vec{\boldsymbol{r}}(n)\cdot\vec{\boldsymbol{r}}(n+n')\rangle, \tag{5.1}$$

where the cross terms in Eq. (5.1) contain the statistical correlation neglected by our MFA. At low loadings, the availability of symmetrically arranged target sites causes the average of these cross terms to vanish. When a molecule executes a jump at higher loadings, however, it leaves behind a vacancy that is likely to be occupied by a successive jump. Thus the correlation of successive jump directions at high loading gives a nonvanishing average of the cross terms in Eq. (5.1).

We can make progress with Eq. (5.1) by noting that at loadings above 32 molecules per unit cell, the MSD for a given molecule is almost exclusively a consequence of W $\rightarrow$W jumps. As such, we can picture diffusion as proceeding on a lattice composed only of W sites. The error generated by this approach, as compared to a more rigorous treatment including all types of jumps, is less than one part in a thousand for 47 molecules per unit cell at $T=300$ K. The diffusion coefficient is then expressed as the product of an MFA diffusivity and a correlation factor, i.e., $D=D_{\mathrm{MFA}}\cdot f$. The MFA diffusivity is given by

$$D_{\mathrm{MFA}}\equiv\lim_{N,t\rightarrow\infty}\frac{1}{6t}\sum_{n=1}^{N}\langle|\vec{\boldsymbol{r}}(n)|^2\rangle = \lim_{N,t\rightarrow\infty}\frac{1}{6t}\sum_{n=1}^{N}a_{11}^2=\frac{Na_{11}^2}{6t}, \tag{5.2}$$

where $a_{11} = 8.79$ Å is the W→W jump distance. The first equality in Eq. (5.2) arises because only W→W jumps are considered. In Eq. (5.2), N is the average number of W→W jumps for each molecule in time t. For 47 molecules per unit cell, it is straightforward to show that $(N/t)_{\mathrm{MFA}} = \frac{6}{16} \cdot \frac{15}{47} \cdot k_{1\to 1}$, where $k_{1\to 1}$ is the fundamental W→W jump rate coefficient. The correlation factor takes the form:

$$f = 1 + 2 \frac{\sum_{n=1}^{N} \sum_{n'=1}^{\infty} \langle \vec{r}(n) \cdot \vec{r}(n+n') \rangle}{\sum_{n=1}^{N} \langle |\vec{r}(n)|^2 \rangle}, \tag{5.3}$$

where we have extended the summation over n' to infinity, since correlation effects decrease very rapidly as n' increases. Due to the symmetry of the lattice, the classic expression for the correlation factor is obtained:[1]

$$f = \frac{1 + \langle \cos\, \theta_1 \rangle}{1 - \langle \cos\, \theta_1 \rangle}, \tag{5.4}$$

where $\langle \cos\, \theta_1 \rangle$ is the average angle between a W→W jump vector of a given molecule and the immediately following W→W jump vector for the same molecule. This analysis is valid whenever the mean square displacement is made up only of W→W jumps. A similar expression can also be obtained in the general case, where all four types of jumps are considered.[29] However, since we will only calculate the correlation factor at infinite vacancy dilution, we will not derive this more complicated expression.

The correlation factor should not display any temperature dependence, as long as the $S_{II}\to S_{II}$ and $S_{II}\leftrightarrow W$ jumps can be neglected. This is because the present treatment only considers W→W jumps, and hence only a single jump rate coefficient. The temperature dependence of $f = D/D_{\mathrm{MFA}}$ would thus cancel for a system with only a single time scale. This helps to explain why $\mathscr{E}_{\mathrm{MFA}}$ in Fig. 8 is nearly temperature independent. We can determine correlation factors from the KMC simulations with 47 molecules per unit cell according to $D_{\mathrm{KMC}}/D_{\mathrm{MFA}}$. The results are 0.631 at 300 K and 0.667 at 400 K. Since the statistical errors in these KMC diffusivities are ca. 8%–10%, these simulated correlation factors are statistically identical, validating the neglect of $S_{II}\leftrightarrow S_{II}$ and $S_{II}\leftrightarrow W$ jumps.

Correlation factors have been calculated analytically for a number of different lattice geometries.[29] We are not aware of values given for the particular tetrahedral arrangement of W sites corresponding to benzene diffusion in Na–Y, which is sketched in Fig. 9. Among the possible methods for calculating f, we used a simplified expression of the original combinatorial method of Bardeen and Herring.[28] Indeed, the low precision of the Monte Carlo calculation, and the fast convergence of the sums due to the lattice connectivity, allows us to limit the summation thus rendering this method both easy to apply and physically meaningful. When periodic boundary conditions are considered, we used the matrix approach to calculate exactly the expectation value of the correlation factor.[29]

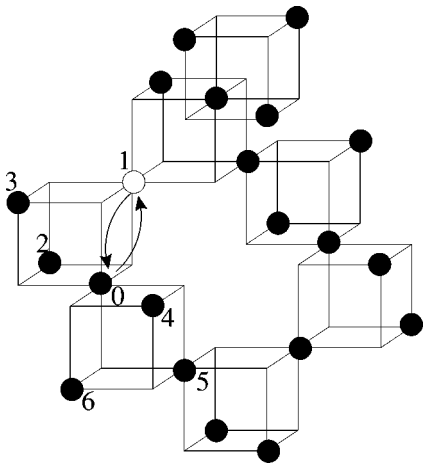

FIG. 9. Lattice of window sites at infinite vacancy dilution; cubes represent Na–Y supercages.

Let us suppose that, as in Fig. 9, a molecule has jumped from the site labeled 1 to the site labeled 0. The average angle between this jump and the next jump of the same molecule will depend on the site from which the vacancy next exchanges with this molecule. Let us write $p(i)$ as the cumulative probability to find the vacancy at site i, such that $p(i) = \Sigma_{j=0}^{\infty} p_j(i)$, where $p_j(i)$ represents the probability to find the vacancy at site i after j jumps. Given a simple choice of axis system, we obtain $\langle \cos\theta_1 \rangle = [-p(1) - p(2) + p(4) + p(6)]/6$. After a few jumps, the probability to find the vacancy at a given site on an infinite lattice will tend to zero, and further will be the same for any site. As such, in the calculation of $p(i)$ we need only consider a very small number of jumps. Note that we must consider at least four jumps, from the initial vacancy site 1, to populate sites 4 to 6. Limiting ourselves to three jumps, we find $\langle \cos\theta_1 \rangle = -0.231$, from whence $f = 0.625$, a result very close to the simulated value. Calculating f with four jumps gives a very similar result.

As indicated before, the KMC simulations have been performed on a lattice of sites containing eight supercages with periodic boundary conditions. The relatively small simulation cell and the periodic boundary conditions slightly change the site populations, as compared to the infinite lattice assumed in the previous paragraph. However, since the simulation cell only contains 16 W sites, it is easy to treat the exact connectivities, and therefore to obtain the relative populations $p(i)$ without limiting to only a few steps. This approach gives a correlation factor that should match more closely the simulated ones. Indeed, the value of 0.641 we find by writing the populations of all 16 W sites comes very close to the KMC values 0.631 and 0.667.

VI. CONCLUDING REMARKS

We have performed kinetic Monte Carlo (KMC) simulations of benzene tracer diffusion in Na–Y at finite loadings for various temperatures to test the analytical diffusion

theory presented in Paper I.[18] Our theory and simulations assume that benzene molecules jump among S_{II} and W sites, located near Na^+ ions in 6-rings and in 12-ring windows, respectively. Our diffusion theory is based on a mean field approximation (MFA) which assumes that instantaneous benzene occupancies in different Na–Y supercages are identical. This yields $D_\theta = \frac{1}{6}k_\theta a_\theta^2$, where $a_\theta \cong 11$ Å is the mean intercage jump length and $1/k_\theta$ is the mean supercage residence time. In Paper I we obtain an analytical expression for k_θ by assuming that S_{II} and W site occupancies are either 0 or 1 and that benzenes do not otherwise interact. For consistency, the KMC simulations presented above use fundamental hopping rate coefficients calculated at infinite dilution.

KMC simulations of $D(\theta)$, k_θ, and a_θ at 300 and 400 K show that our MFA is essentially exact for loadings that allow S_{II} site vacancies, and that the concentration dependence is controlled by k_θ. For higher loadings, the MFA error is independent of temperature, and increases roughly linearly with loading to a maximum value of ca. 25%. This error arises because the MFA neglects statistical correlation between jumps when, e.g., a random walker jumps into a W site separating nearly empty and full cages. We present an analytical theory for such correlated motion at infinite vacancy dilution, which predicts the corresponding KMC simulated diffusivities to within statistical Monte Carlo error.

We have thus developed a useful, approximate model for benzene tracer diffusion in Na–Y, from which we have derived simple analytical formulas revealing the temperature and concentration dependence of the diffusivity. These formulas have shown semiquantitative agreement with kinetic Monte Carlo simulations using rate parameters consistent with those in the theory. Further study is required to determine how widely applicable the approach presented above is to transport problems in other host–guest systems, such as modeling tracer diffusion of other guests or modeling diffusion in other zeolites such as silicalite.[36] Regarding other guest species, our present approach is useful when guests diffuse through zeolites by making infrequent, uncorrelated jumps among relatively deep sorption sites. Regarding diffusion in silicalite, channel intersections are analogous to Na–Y supercages, while channels are analogous to W sites connecting adjacent supercages. As such, our approach should be applicable to studying mobility in MFI type zeolites.

Since analytical theories can often display the physics essential to a process more clearly than simulations, and are certainly more desirable in terms of computational effort, it is important to extend the results presented herein to include the effects of medium to long range guest–guest interactions.[37,38] We will address the importance of these interactions in a forthcoming publication[25] by considering how nearest neighbor S_{II} and W site occupancies affect binding site stabilities and residence times.

TABLE I. Levels of theory in Fig. 7.

Level of theory	Description
MFA1	$D(\theta) = \frac{1}{6}k_\theta a_\theta^2$, $a_\theta = 11$ Å, k_θ from Eqs. (2.1) and (2.3)
MFA2	$D(\theta) = \frac{1}{6}k_\theta a_\theta^2$, a_θ and k_θ from KMC
MSD	$D(\theta) = \lim_{t\to\infty}\langle \mathscr{R}^2(t)\rangle/6t$ from KMC

ACKNOWLEDGMENTS

The authors acknowledge excellent suggestions from the reviewer. S.M.A. acknowledges support from the NSF under Grants No. CHE-9625735 and No. CHE-9616019, and from Molecular Simulations, Inc. for generously providing visualization software. Acknowledgment is made to the donors of the Petroleum Research Fund, administered by the American Chemical Society, for partial support of this research under Grant No. ACS-PRF 30853-G5.

[1] J. Kärger and D. M. Ruthven, *Diffusion in Zeolites and Other Microporous Solids* (Wiley, New York, 1992).
[2] N. Y. Chen, T. F. Degnan, Jr., and C. M. Smith, *Molecular Transport and Reaction in Zeolites* (VCH, New York, 1994).
[3] J. Weitkamp, in *Catalysis and Adsorption by Zeolites*, edited by G. Olhmann, J. C. Vedrine, and P. A. Jacobs (Elsevier, Amsterdam, 1991).
[4] J. M. Newsam, ''Zeolites,'' in *Solid State Chemistry: Compounds*, edited by A. K. Cheetham and P. Day (Oxford University Press, Oxford, 1992), pp. 234–280.
[5] P. Demontis, S. Yashonath, and M. L. Klein, J. Phys. Chem. **93**, 5016 (1989).
[6] L. M. Bull, N. J. Henson, A. K. Cheetham, J. M. Newsam, and S. J. Heyes, J. Phys. Chem. **97**, 11776 (1993).
[7] D. Barthomeuf and B. H. Ha, J. Chem. Soc., Faraday Trans. **69**, 2158 (1973).
[8] A. N. Fitch, H. Jobic, and A. Renouprez, J. Phys. Chem. **90**, 1311 (1986).
[9] L. Uytterhoeven, D. Dompas, and W. J. Mortier, J. Chem. Soc., Faraday Trans. **88**, 2753 (1992).
[10] H. Klein, C. Kirschhock, and H. Fuess, J. Phys. Chem. **98**, 12345 (1994).
[11] P. J. O'Malley and C. J. Braithwaite, Zeolites **15**, 198 (1995).
[12] S. M. Auerbach, N. J. Henson, A. K. Cheetham, and H. I. Metiu, J. Phys. Chem. **99**, 10600 (1995).
[13] J. Kärger and D. M. Ruthven, Stud. Surf. Sci. Catal. **105**, 1843 (1997).
[14] S. M. Auerbach and H. I. Metiu, J. Chem. Phys. **105**, 3753 (1996).
[15] S. M. Auerbach, L. M. Bull, N. J. Henson, H. I. Metiu, and A. K. Cheetham, J. Phys. Chem. **100**, 5923 (1996).
[16] S. M. Auerbach and H. I. Metiu, J. Chem. Phys. **106**, 2893 (1997).
[17] S. M. Auerbach, J. Chem. Phys. **106**, 7810 (1997).
[18] C. Saravanan and S. M. Auerbach, J. Chem. Phys. **107**, 8120 (1997).
[19] C. Saravanan and S. M. Auerbach, J. Chem. Phys. **107**, 8132 (1997).
[20] F. Jousse and S. M. Auerbach, J. Chem. Phys. **107**, 9629 (1997).
[21] R. L. June, A. T. Bell, and D. N. Theodorou, J. Phys. Chem. **95**, 8866 (1991).
[22] K. A. Fichthorn and W. H. Weinberg, J. Chem. Phys. **95**, 1090 (1991).
[23] A. Germanus, J. Kärger, H. Pfeifer, N. N. Samulevic, and S. P. Zdanov, Zeolites **5**, 91 (1985).
[24] D. Stauffer and A. Aharony, *Introduction to Percolation Theory* (Taylor & Francis, Bristol, PA, 1991).
[25] C. Saravanan and S. M. Auerbach (in preparation).
[26] S. Brandani, Z. Xu, and D. Ruthven, Microporous Mater. **7**, 323 (1996).
[27] D. M. Shen and L. V. C. Rees, Zeolites **11**, 666 (1991).
[28] J. Bardeen and C. Herring, in *Atom Movements* (American Society for Metals, Cleveland, 1951), p. 87.
[29] A. D. Le Claire, in *Physical Chemistry: An Advanced Treatise, Volume X*, edited by W. Jost (Academic, New York, 1970), p. 261.
[30] G. E. Murch, in *Diffusion in Crystalline Solids*, edited by G. E. Murch and A. S. Nowick (Academic, Orlando, 1984), p. 379.
[31] R. J. Borg and G. J. Dienes, *An Introduction to Solid State Diffusion* (Academic, San Diego, 1988).

[32] P. Benoist, J.-L. Bocquet, and P. Lafore, Acta Metall. **25**, 265 (1977).
[33] I. V. Belova and G. E. Murch, Defect Diffus. Forum **143**, 291 (1997).
[34] D. Wolf, in *NATO ASI Series B: Physics – Mass Transport in Solids*, edited by F. Bénière and C. R. A. Catlow (Plenum, New York, 1983), p. 149.
[35] M. Koiwa, J. Phys. Soc. Jpn. **45**, 1327 (1978).
[36] R. Q. Snurr, A. T. Bell, and D. N. Theodorou, J. Phys. Chem. **98**, 11948 (1994).
[37] D. S. Sholl and K. A. Fichthorn, Phys. Rev. Lett. (to be published).
[38] C. Rodenbeck, J. Kärger, and K. Hahn, Phys. Rev. E **55**, 5697 (1997).